Original Article

The Impact of Point Spread Function Modeling on Scan Duration in PET Imaging

Sahar Ahangari[1, 2], Pardis Ghafarian[3, 4, *], Mahnaz Shekari[1, 2], Hossein Ghadiri[1, 2], Mehrdad Bakhshayeshkaram[3, 4], and Mohammad Reza Ay[1, 2]

1- Department of Medical Physics and Biomedical Engineering, Tehran University of Medical Sciences, Tehran, Iran.

2- Research Center for Molecular and Cellular Imaging, Tehran University of Medical Sciences, Tehran, Iran.

3- Chronic Respiratory Diseases Research Center, National Research Institute of Tuberculosis and Lung Diseases (NRITLD), Shahid Beheshti University of Medical Sciences, Tehran, Iran.

4- PET/CT and Cyclotron Center, Masih Daneshvari Hospital, Shahid Beheshti University of Medical Sciences, Tehran, Iran.

Received: 4 September 2015
Accepted: 30 October 2015

ABSTRACT

Purpose- In this study, we investigated the impact of PSF reconstruction on the PET acquisition time. Additionally, we evaluated whether a reduction in acquisition time would compromise the accuracy of quantitative measures using PSF algorithm.

Methods- Both phantom and patient images were evaluated. A complete set of experiments were performed using an image quality phantom containing 6 inserts with 4:1 lesion to background ratio. Whole-body FDG PET/CT scan of 17 patients with different primary cancers were used in this study. All phantom images reconstructed with 3 iterations, 24 subsets for 180, 150, 120, 90, and 60 s acquisition time per bed position. Post-smoothing filters with FWHM of 5 and 4 mm applied to HD and HD+PSF images respectively. Clinical PET images reconstructed with 3 iterations and 18 subsets. Quantitative analysis performed by CV%, SNR, RC, and SUV_{max}.

Results- By incorporating PSF algorithm, CV decreased 11.1% and 17.01%±0.92% for both phantom and clinical images. In addition, better edge detection achieved specially for smaller focal points. It was shown by reconstructing images with PSF algorithm, acquisition time can be reduced 33.3% with no significant changes of image quality and quantitative accuracy (P-value<0.05).

Conclusion- It can be concluded that using PSF algorithm improves the image quality, lesion detection, and quantitative accuracy. Besides, by incorporating this algorithm, the acquisition time can be reduced with no loss of image quality and quantitative accuracy where it is possible to have higher patient throughout with the same image quality.

Keywords:
PET,
PSF Modeling,
Acquisition Time,
SNR.

1. Introduction

^{18}F-FDG PET/CT has become a standard equipment and highly sensitive method which provides comprehensive and reliable information especially in oncology to stage cancer and metastatic diseases in a wide variety of tumors. It can provide a combination of anatomical and functional information that helps in making more accurate diagnoses [1-4]. High image quality is compulsory for an accurate diagnosis, although spatial resolution of PET images are relatively poor in comparison to other imaging modalities

Corresponding Author:
Pardis Ghafarian, PhD
Shahid Beheshti University of Medical Sciences, Masih Daneshvari Hospital, Tehran, Iran.
Tel: (+98) 2166907532
Email: pardis.ghafarian@sbmu.ac.ir

[5]. Higher count statistic acquisitions can result in image quality improvements and an increased accuracy in SUV estimations [6]. Due to these reasons, PET/CT is a prolonged examination, and achieving an acceptable clinical image quality is still a controversial issue, particularly in orthopedic and pediatric patients [7].

Recently, major developments have been implemented in PET imaging. In particular, advanced reconstruction algorithms that model the point spread function (PSF) of a system have recently become commercially available to recover the degradation of the spatial resolution due to physical factors (e.g., positron range, noncollinearity, inter-crystal penetration) [8-10]. To compensate for this distortion, PSFs are measured at several points in the FOV using a point source. The measured PSFs are then incorporated into the reconstruction algorithm which lead to position the line of responses in their actual geometric location. It was shown that this algorithm improves both the spatial resolution and noise level of reconstructed PET images [11]. Considering that newer generation clinical PET systems equipped with such algorithms, related studies of lesion-detection in PSF reconstruction have been performed using phantoms [12] and clinical data [13]. PSF reconstruction improves spatial resolution throughout the entire field of view (FOV), diminishes PVE and leads to a better image quality and lesion detection, especially in the detection of small lesions at large radial distances [14].

In this study, we investigated the impact of PSF reconstruction on PET scan duration while trying to keep image quality and quantitative accuracy. As the typical scanning time for whole-body PET imaging lasts almost 30 to 45 min, the acquisition time per bed position plays an important role in PET imaging [15]. Thus, reducing the scanning time could be effective in promoting patient comfort and the cost-effectiveness of the examination. Hence, the potential application of PSF algorithm on reducing scan duration, which can be translated to dose reduction, was assessed by evaluating the accuracy of quantitative values, lesion detectability and image quality on phantom and clinical images.

2. Materials and Methods

2.1. PET/CT Scanner

The scanner used in this study, was a PET/CT GE Discovery 690 with 64-slice CT. The PET scanner has 24 detector rings made of LYSO crystals that provide 47 trans-axial plans with a slice thickness of 2.7 mm. In total, it has 13824 crystals covering an axial FOV of 15.7 cm and a trans-axial FOV of 70 cm in diameter. Its coincidence time window is 4.1 ns. The scanner is equipped with High Definition algorithm (HD) and PSF modeling (which is commercially named SharpIR algorithm).

2.2. Data Acquisition

Phantom specifications

The NEMA IEC Body Phantom consists of six inserts with internal diameters of 10, 13, 17, 22, 28, and 37 mm, simulating tumors of varying sizes was used in this study (Figure 1). In addition, it was consisted of a cylindrical insert filled with low-atomic-number material (polystyrene with density of 0.3 ± 0.1 g/ml) to simulate lung attenuation. The injected activity for standard patients (≈70 kg) in our clinic was usually 370 MBq of FDG, resulting in a background activity concentration of 5.3 kBq/ml. The activity concentrations in the cylindrical inserts were chosen in order to have a lesion to background ratio (LBR) of 4:1. The data acquisition was performed in 3-dimensional (3D) list mode for 5 minutes per bed position. In list mode acquisition, events record as a list of data consisting of the spatial coordinates of interaction, the energy value, and the time of interaction.

Figure 1. The prepared phantom on the bed of the PET/CT scanner ready for scanning. All inserts filled with F-18 activity.

Patient Population

17 patients (9 men and 8 women) with 105 lesions were included in this study. The average weight of the patients was 78.4±15.6 kg (BMI: 27.49±5.46). All patients fasted 6 h before undergoing PET/CT examination. They received 5.29±0.11 MBq/kg of [18F] FDG and were scanned 60 minutes after an intravenous injection. After that, a whole body CT scan with 120 kVp and 100 mA was performed. The PET acquisitions were done using seven to ten bed positions to cover the area from mid-thigh to the top of the head. Acquisition time for all patients was 3 min per bed position.

2.3. Reconstruction Methods

To evaluate the impact of reducing scan duration by using list-mode data, phantom images were reconstructed for different times per bed position. Acquisition times was reduced from 180 to 60 second per bed position (180, 150, 120, 90, and 60 s). Phantom images reconstructed with 3 iterations and 24 subsets for HD and HD+PSF algorithms. The full width at half maximum (FWHM) of Gaussian filter was 5 mm for HD algorithm and 4 mm for images reconstructed with PSF algorithm.

A clinical study was conducted to evaluate the potential application of PSF-modeling on reducing scan time. All clinical PET data were, then, reconstructed with HD+PSF algorithm, 3 iterations and 18 subsets. The FWHM of the Gaussian filter was 6.4 mm for all cases. All data were reconstructed into a 256×256 matrix with a 2.7 mm pixel size.

2.4. Data Analysis

The evaluation of PET image quality was performed by calculating the coefficient of variance (CV) in the background and signal to noise ratio (SNR). 2D ROIs over slices suggested in NEMA NU-2 instructions [16] were used in our study. We placed 12 circular ROIs of 37 mm in diameter on the central slice and on slices ±1 cm and ±2 cm away from the central one (total of 60 ROIs). For clinical data as shown in Figure 2, the 3 circular ROIs with 30 mm in diameter were placed on 3 contiguous axial slices in the largest liver section. CV% were defined as below:

$$CV\% = SD_{BG} / C_{BG} \times 100\% \quad (1)$$

Where the SD_{BG} was the standard deviation of the background ROIs and C_{BG} was the average activity in the background ROIs.

To calculate the SNR of each focal point, a VOI was drawn which covered the entire volume of the focal point.

$$SNR=(C_{Max,L} - C_{BG}) / SD_{BG} \quad (2)$$

Where the $C_{max,L}$ refers to maximum activity concentration within a lesion VOI.

A quantitative analysis of the images were performed by calculating SUV and recovery coefficient of activity concentration (RC %). The SUV_{max} is now probably the most widely used method for the quantification of 18F-FDG PET studies. Based on VOI statistics, SUV_{max} refers to maximum activity concentration within a VOI. All SUV measurements were normalized to the body weight of the patient and computed as:

$$SUV_{max} = \frac{tumour\ activity(Bq/ml) \times body\ weight(g)}{injected\ dose\ (Bq)} \quad (3)$$

To evaluate the accuracy of measured activity concentration, RC was defined as:

$$RC\% = C_{measured} / A_{known} \times 100\% \quad (4)$$

Where $A_{measured}$ was the measured activity concentration in the insert, and A_{known} was the known activity concentration in the same region.

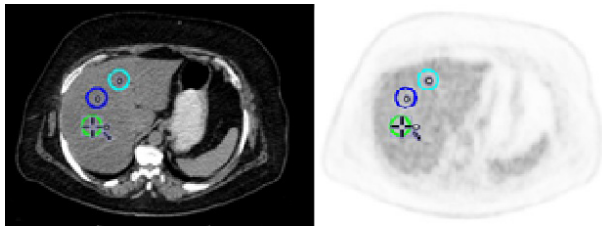

Figure 2. Three circular ROIs with 30 mm in diameter were placed on 3 contiguous axial slices of CT (left) and PET images (right).

2.5. Statistics

All statistical analysis were performed using SPSS Statistics Version 21. P-value <0.05 was considered statistically significant. The CV_{liver} and SNR of each reconstruction method were compared using paired t-test. Repeated measurement ANOVA test was additionally performed to calculate the difference between relative differences of SUV for different scan times.

3. Results

Figure 3 shows the transverse slice of IQ phantom PET images at 5.3 kBq/ml background activity level reconstructed by HD and HD+PSF algorithms. PSF modeling yielded slight improvement in edge definition especially in smallest insert. To compare the resultant image quality of both algorithms, CV% and SNR were assessed. Background uniformity was higher in images reconstructed with PSF algorithm. In addition, it yielded more robust SNR for all inserts (Figure 4).

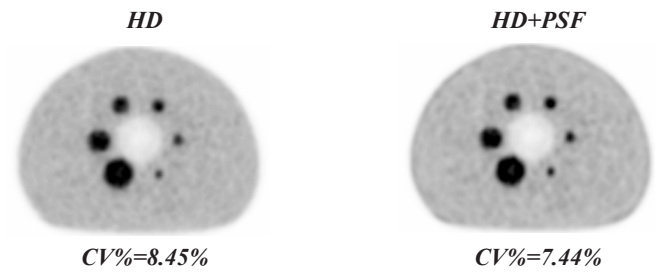

Figure 3. Phantom images reconstructed with HD (left) and HD+PSF (right) algorithm, 3 iterations, and 24 subsets. The FWHM of Gaussian filter was 5 mm for HD algorithm and 4 mm for PSF algorithm.

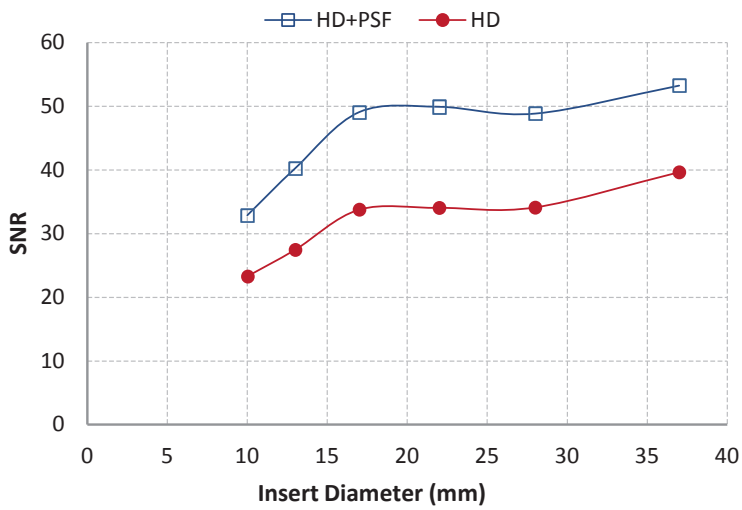

Figure 4. SNR was calculated for all inserts to compare resultant image quality of HD and HD+PSF algorithms.

In order to determine the impact of PSF algorithm on image quality of clinical images, CV_{liver} and SNR calculated for images reconstructed with HD and HD+PSF algorithms. CV_{liver}, as a key factor of image quality, was superior to that of HD images (P-value<0.0001). SNR of focal points for PSF algorithm versus HD algorithm was plotted by Bland-Altman method (Figure 5). For all focal points, SNR for images reconstructed with PSF modelling were above the line of equality, which confirmed SNR enhancement by PSF algorithm.

Within assessing PSF performance, the possibility of reducing acquisition time was evaluated. Figure 6 showed phantom images reconstructed with PSF algorithm which resulted less noise level and superior image quality compared to those without PSF, for all acquisition times.

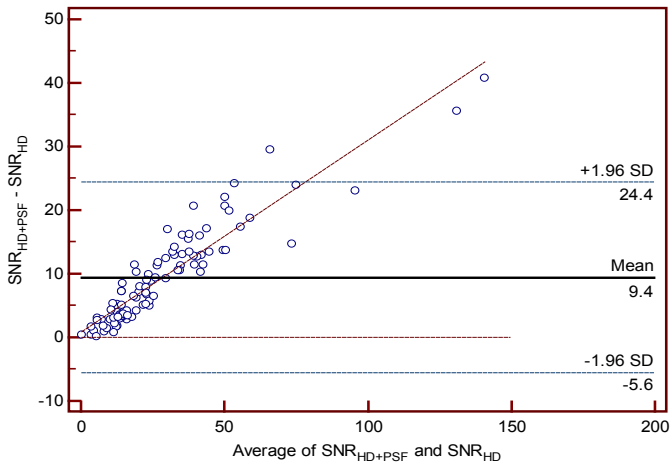

Figure 5. Bland-Altman plot for comparing resultant SNR of HD and HD+PSF algorithms.

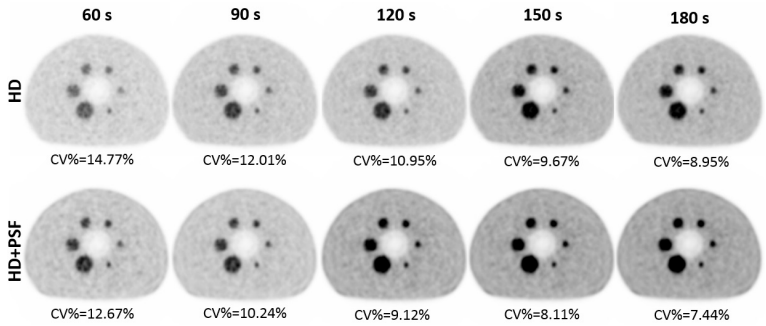

Figure 6. Transverse images of the Image Quality phantom for different acquisition times. The reconstruction parameters were iterations and subsets 3 × 24. FWHM of Gaussian filter was 5 mm for HD and 4 mm for HD+PSF algorithm.

The $SNR_{10\ mm}$ was plotted versus CV as a function of acquisition time. In Figure 7, the Trade off between $SNR_{10\ mm}$ and CV showed that at equivalent noise level, image reconstructed with PSF modeling for 120 s acquisition time yielded superior SNR in comparison with image reconstructed with HD algorithm for 180 s. RCs of smallest insert for images with matched voxel noise level, as an indicator of quantitative accuracy, were 51.8% and 55.8% (HD 180 s and HD+PSF 120 s respectively). It showed that more accurate quantification was achieved by PSF algorithm, even in shorter acquisition time.

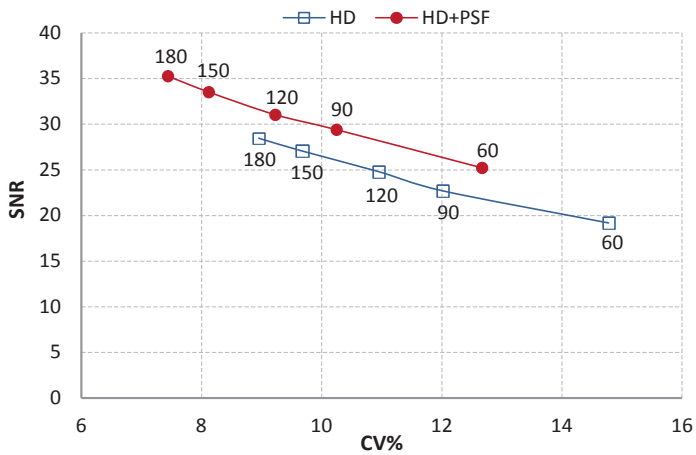

Figure 7. The relationship between the CV% and the SNR for HD and HD+PSF algorithms in different acquisition times per bed position (60, 90, 120, 150, and 180 s).

Figure 8 demonstrated by decreasing scan time, CV_{liver} increased for images reconstructed with HD+PSF algorithms. It was shown by decreasing acquisition time to 120 s, an acceptable clinical noise level was achieved (CV_{liver}<10%) [17]. SUV_{max} for 150, 120, 90, and 60 s versus SUV_{max} (180 s) were plotted (Figure 9). In comparison with 180 s acquisition time, SUV_{max} changes were not statistically significant by decreasing the acquisition time to 120 s (P-value>0.05). Figure 10 shows clinical examples of PET images reconstructed with PSF algorithm for different scan times. In these clinical images, SUV_{max} of lesions did not change significantly, and CV was clinically acceptable for 120 s acquisition time.

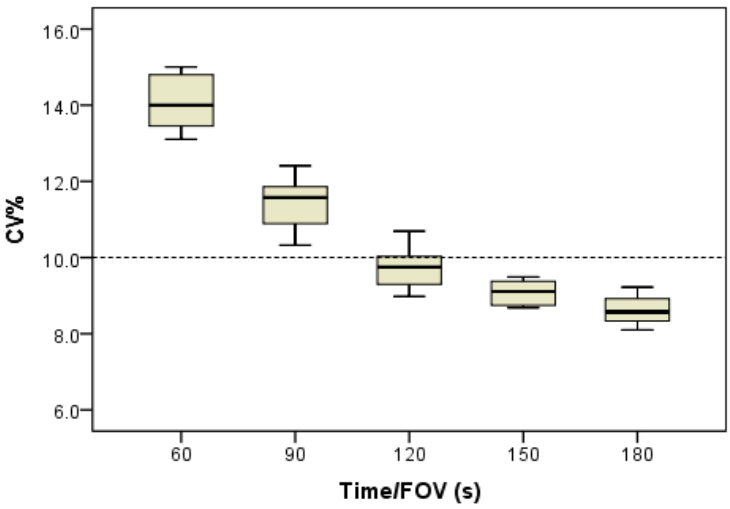

Figure 8. CV% of clinical PET images reconstructed with HD+PSF algorithm for different acquisition times.

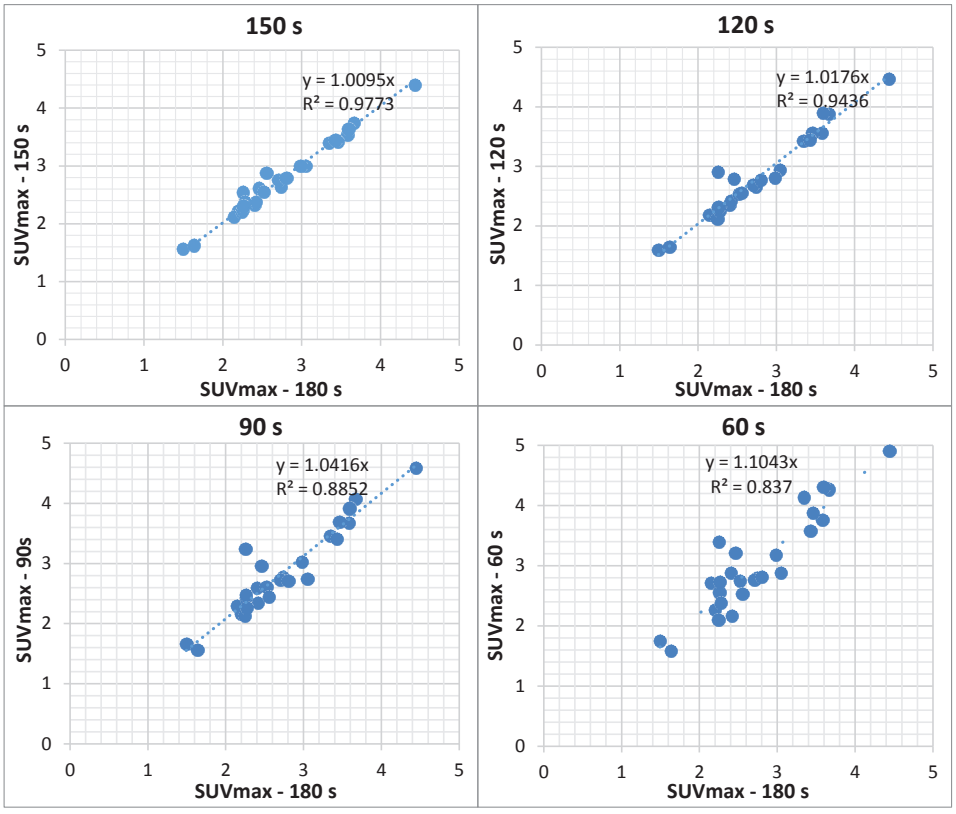

Figure 9. SUV_{max} of different acquisition times versus SUV_{max} of 180 s acquisition time for focal points.

4. Discussion

It is well known that the assessment of new technologies that are implemented in PET imaging is essential. Some of them such as advanced reconstruction algorithms are likely to not only improve the diagnostic performance, but also change the quantification and image features. PSF reconstruction is a new reconstruction algorithm which improves the spatial resolution and is therefore expected to lead to the detection of smaller metastases than can be achieved by conventional algorithms [8].

In this study, we evaluated the effect of PSF modeling on image quality and quantitative accuracy. By using PSF algorithm, CV decreased to 11.1% and 17.01%±0.92% for phantom and clinical images respectively. Images reconstructed with PSF yielded to a better background uniformity [11] and a better edge detection specially for smaller inserts [13]. Besides, by using this new algorithm, SNR enhanced 42.88%±1.93% for all inserts [14, 18]. As previous studies showed, the image uniformity and SNR were improved for clinical images reconstructed with PSF algorithm [19]. Bland-Altman plot demonstrated that SNR for images reconstructed with PSF modelling were above line of equality, which can be interpreted as SNR enhancement. In addition, PSF algorithm performance was superior for focal points with higher SNR values in comparison to that of poor SNR.

As image quality improved, the feasibility of reducing acquisition time was assessed. The suggested acquisition time per bed position used in the clinical setup for diagnostic and oncological use is between 2 to 5 min [20, 21]. Detailed work regarding this issue is addressed by Duran *et al.* [22]. By increasing the acquisition time and subsequently increasing counts, CV decreased for both algorithms. It should be noted that by decreasing scan time, due to loss of counts, insert's signal decreased which degraded the visual quality of images. Our phantom study showed that by incorporating PSF algorithm, acquisition time can be reduced to 120 s, with maintaining image quality acceptable. The impact of reducing acquisition time on quantitative accuracy, as a critical factor in clinical decision, showed no bias on RC of all inserts for images reconstructed with PSF algorithm, with shorter acquisition time. In other words, the quantitative accuracy improved by 8.56%±091%, which was shown previously by Hausmann *et al.*[23].

For images reconstructed with PSF algorithm, acquisition time can be reduced 33.3% with no significant changes of image quality and quantitative accuracy (P-value<0.05). Slope of Regression lines for SUV_{max} in reduced scan time was 1 which can be considered as no changes in accuracy of SUV_{max}, as an important factor for tumor staging. As a clinical reference, Figure 10 shows by reducing acquisition time even to 90 s, an acceptable image quality is achieved with no bias in SUV_{max}.

PSF algorithm improves the image quality, lesion detection, and quantitative accuracy. Besides, by incorporating this algorithm, acquisition time can be reduced to 120 s with no loss of image quality and quantitative accuracy. In clinical scan, it can lead to decreasing the acquisition time up to 10 min. This time reduction can be translated into reducing injected dose especially for patients with PET series imaging and follow up.

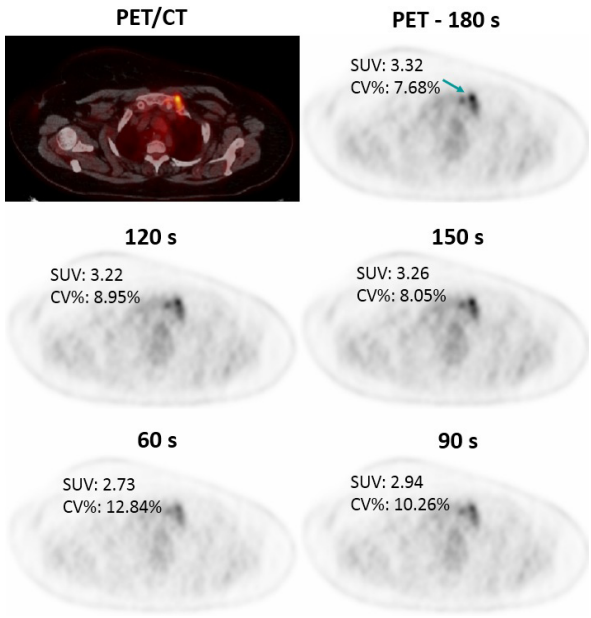

Figure 10. Transversal view of patient PET images reconstructed in different acquisition time.

Acknowledgment

This work supported by Tehran University of Medical Sciences, Tehran, Iran under grant No. 26840 and Masih Daneshvari Hospital, Shahid Behehsti University of Medical Sciences, under grant No. 714/10019. We would like to thank the staff at the Department of PET/CT and Cyclotron Center in Masih Daneshvari Hospital for their valuable clinical support.

References

1- E. M. Rohren, T. G. Turkington, and R. E. Coleman, "Clinical applications of PET in oncology 1," *Radiology,* vol. 231, pp. 305-332, 2004.

2- B. M. Fischer, J. Mortensen, and L. Højgaard, "Positron emission tomography in the diagnosis and staging of lung cancer: a systematic, quantitative review," *The lancet oncology,* vol. 2, pp. 659-666, 2001.

3- D. Groheux, S. Giacchetti, M. Delord, E. Hindié, L. Vercellino, C. Cuvier, *et al.*, "18F-FDG PET/CT in staging patients with locally advanced or inflammatory breast cancer: comparison to conventional staging," *Journal of Nuclear Medicine,* vol. 54, pp. 5-11, 2013.

4- J. W. Fletcher, B. Djulbegovic, H. P. Soares, B. A. Siegel, V. J. Lowe, G. H. Lyman, *et al.*, "Recommendations on the use of 18F-FDG PET in oncology," *Journal of Nuclear Medicine,* vol. 49, pp. 480-508, 2008.

5- Y. Masuda, C. Kondo, Y. Matsuo, M. Uetani, and K. Kusakabe, "Comparison of imaging protocols for 18F-FDG PET/CT in overweight patients: optimizing scan duration versus administered dose," *Journal of Nuclear Medicine,* vol. 50, pp. 844-848, 2009.

6- R. Boellaard, "Standards for PET Image Acquisition and Quantitative Data Analysis," *Journal of Nuclear Medicine,* vol. 50, pp. 11S-20S, 2009.

7- D. J. Kadrmas, T. J. Bradshaw, M. E. Casey, and J. J. Hamill, "Scan time reduction with advanced PET reconstruction: Preserving lesion detection performance," in *Nuclear Science Symposium Conference Record (NSS/MIC), 2010 IEEE*, 2010, pp. 2381-2387.

8- A. M. Alessio, C. W. Stearns, S. Tong, S. G. Ross, S. Kohlmyer, A. Ganin, *et al.*, "Application and evaluation of a measured spatially variant system model for PET image reconstruction," *Medical Imaging, IEEE Transactions on,* vol. 29, pp. 938-949, 2010.

9- F. L. Andersen, T. L. Klausen, A. Loft, T. Beyer, and S. Holm, "Clinical evaluation of PET image reconstruction using a spatial resolution model," *Eur J Radiol,* vol. 82, pp. 862-9, May 2013.

10- C. Lasnon, R. J. Hicks, J.-M. Beauregard, A. Milner, M. Paciencia, A.-V. Guizard, *et al.*, "Impact of point spread function reconstruction on thoracic lymph node staging with 18F-FDG PET/CT in non–small cell lung cancer," *Clinical nuclear medicine,* vol. 37, pp. 971-976, 2012.

11- V. Y. Panin, F. Kehren, C. Michel, and M. Casey, "Fully 3-D PET reconstruction with system matrix derived from point source measurements," *Medical Imaging, IEEE Transactions on,* vol. 25, pp. 907-921, 2006.

12- G. Akamatsu, K. Ishikawa, K. Mitsumoto, T. Taniguchi, N. Ohya, S. Baba, *et al.*, "Improvement in PET/CT Image Quality with a Combination of Point-Spread Function and Time-of-Flight in Relation to Reconstruction Parameters," *Journal of Nuclear Medicine,* vol. 53, pp. 1716-1722, 2012.

13- G. Akamatsu, K. Mitsumoto, T. Taniguchi, Y. Tsutsui, S. Baba, and M. Sasaki, "Influences of point-spread function and time-of-flight reconstructions on standardized uptake value of lymph node metastases in FDG-PET," *European Journal of Radiology,* vol. 83, pp. 226-230, 2014.

14- S. Tong, A. M. Alessio, and P. E. Kinahan, "Noise and signal properties in PSF-based fully 3D PET image reconstruction: an experimental evaluation," *Physics in Medicine and Biology,* vol. 55, pp. 1453-1473, 2010.

15- D. Delbeke, R. E. Coleman, M. J. Guiberteau, M. L. Brown, H. D. Royal, B. A. Siegel, *et al.*, "Procedure guideline for tumor imaging with 18F-FDG PET/CT 1.0," *Journal of Nuclear Medicine,* vol. 47, pp. 885-895, 2006.

16- B. W. Jakoby, Y. Bercier, C. C. Watson, B. Bendriem, and D. W. Townsend, "Performance characteristics of a new LSO PET/CT scanner with extended axial field-of-view and PSF reconstruction," *Nuclear Science, IEEE Transactions on,* vol. 56, pp. 633-639, 2009.

17- H. Fukukita, M. Senda, T. Terauchi, K. Suzuki, H. Daisaki, K. Matsumoto, *et al.*, "Japanese guideline for the oncology FDG-PET/CT data acquisition protocol: synopsis of Version 1.0," *Ann Nucl Med,* vol. 24, pp. 325-34, May 2010.

18- J. Schaefferkoetter, M. Casey, D. Townsend, and G. El Fakhri, "Clinical impact of time-of-flight and point response modeling in PET reconstructions: a lesion detection study," *Physics in medicine and biology,* vol. 58, p. 1465, 2013.

19- K. Thielemans, E. Asma, S. Ahn, R. Manjeshwar, T. Deller, S. Ross*, et al.*, "Impact of PSF modelling on the convergence rate and edge behaviour of EM images in PET," in *Nuclear Science Symposium Conference Record (NSS/MIC), 2010 IEEE*, 2010, pp. 3267-3272.

20- R. Boellaard, M. J. O'Doherty, W. A. Weber, F. M. Mottaghy, M. N. Lonsdale, S. G. Stroobants*, et al.*, "FDG PET and PET/CT: EANM procedure guidelines for tumour PET imaging: version 1.0," *European Journal of Nuclear Medicine and Molecular Imaging,* vol. 37, pp. 181-200, 2009.

21- R. Boellaard, R. Delgado-Bolton, W. J. Oyen, F. Giammarile, K. Tatsch, W. Eschner*, et al.*, "FDG PET/CT: EANM procedure guidelines for tumour imaging: version 2.0," *Eur J Nucl Med Mol Imaging,* vol. 42, pp. 328-54, Feb 2015.

22- F. Molina-Duran, D. Dinter, F. Schoenahl, S. O. Schoenberg, and G. Glatting, "Dependence of image quality on acquisition time for the PET/CT Biograph mCT," *Z Med Phys,* vol. 24, pp. 73-9, Mar 2014.

23- D. Hausmann, D. J. Dinter, M. Sadick, J. Brade, S. O. Schoenberg, and K. Busing, "The impact of acquisition time on image quality in whole-body 18F-FDG PET/CT for cancer staging," *J Nucl Med Technol,* vol. 40, pp. 255-8, Dec 2012.